LUMINOSITY OF EXPERIMENT WITH INTERNAL PELLET TARGET AND MISALINGNED ELECRON BEAM

D.Reistad, A.Smirnov, A.Sidorin, using S-LSR and COSY results
Draft, 15.03.07

Introduction

In the case of pellet target application the pellets crosses the antiproton beam one by one. At the time scale sufficiently longer than the pellet time of flight through the antiproton beam the luminosity can be calculated using a value of effective target thickness. The pellet velocity can be estimated from the pellet generation rate, which is typically equal to 70 – 100 kHz, and mean inter pellet distance, which is about 3 – 5 mm. The velocity lies in the range $(2\div5)\cdot10^2$ m/s. At the time scale comparable with the pellet generation period, which is about 10 μs, the luminosity is varied from zero (when no pellet is inside the beam) to some maximum value corresponding to the pellet position in the maximum of the beam distribution function. (We assume that the vertical beam size is less than inter pellet distance and only one pellet can be inside the beam.) Ratio between maximum and average luminosity is important parameter of the experiment. The choice of the antiproton beam dimensions in the target position has to provide minimum of this parameter.

The luminosity in the case of beam interaction with a uniform internal target at thickness of ρ [Atoms/cm^2] is given by

$$L = \frac{N\rho}{T_{rev}} \tag{1}$$

where N is the number of ions circulating in the ring, T_{rev} is the revolution period. When the target size is less than the beam size one can introduce “effective” target thickness, and for fixed target and beam sizes the luminosity can be calculated with the same formula:

$$L = \frac{N\rho_{eff}}{T_{rev}}. \tag{2}$$

The effective thickness depends on the antiproton beam dimensions and shape of the distribution function.

The goal of the electron cooling application at HESR is to reach antiproton relative momentum spread of the order of 10^{-5}. To avoid longitudinal heating due to intrabeam scattering the antiproton emittance has to be stabilized at the level of 10^{-7} π·m·rad. The beam size required for optimum ratio between maximum and mean luminosity can be obtained by a choice of beta function value in the target position at the level of a few meters.

One of effective ways to stabilize the beam emittance is an introduction of some angle between electron beam axis and equilibrium antiproton orbit in the cooling section. However, if the misalignment angle exceeds some threshold value the antiproton distribution function shape can change dramatically. This effect was called “chromatic instability”. Instead of Gaussian distribution a distribution with well pronounced two peak structure at maximum particle density at the edges of the profile is appearing. This situation corresponds to so called Hopf bifurcation and can lead to increase of the maximum to mean luminosity ratio.

In this note we discuss initially optimum beam size in the target position at typical pellet target parameters and Gaussian distribution of antiprotons. In the second chapter the peculiarity of the particle distribution at cooling with misaligned electron beam and maximum to mean luminosity ratio are described.

1. Gaussian beam

In the case of a single moving pellet the effective target thickness is a function of the pellet position inside the beam. At Gaussian distribution, obviously, a maximum of the effective thickness corresponds to the pellet position in the center of the beam. For a spherical pellet of the radius of r_p located in zero position its length along the trajectory of antiproton with co-ordinates (x, y) is

$$2\sqrt{r_p^2 - x^2 - y^2}\,.$$

Correspondingly for a beam with Gaussian distribution in both transverse planes the effective thickness can be calculated as:

$$\rho_{eff,\max} = \frac{\Re}{2\pi\sigma_x\sigma_y}\int_{-r_p}^{r_p}\int_{-\sqrt{r_p^2-x^2}}^{\sqrt{r_p^2-x^2}} 2\sqrt{r_p^2 - x^2 - y^2}\,\exp\left(-\frac{x^2}{2\sigma_x^2} - \frac{y^2}{2\sigma_y^2}\right)dydx\,, \qquad (3)$$

where $\Re$ = $4.26\cdot10^{22}$ Atoms/cm^3 is the frozen hydrogen density, σ_x and σ_y are horizontal and vertical rms beam dimensions. This formula is valid for the maximum effective thickness when only one pellet crosses the beam in each moment of time, i.e. the vertical beam size is sufficiently less then the mean distance between pellets.

In the first approximation the pellets form a well collimated flux inside which they are distributed almost uniformly in transverse direction and moves in vertical directions divided by some mean distance. The pellet target geometry corresponding to this model is sketched in the Fig. 1.

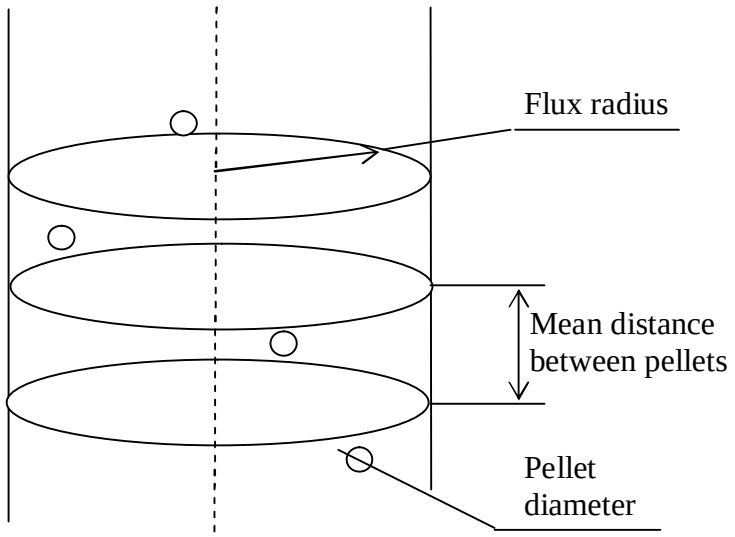

Fig. 1. Schematics of the pellet target geometry. The pellets move in the vertical direction from top to bottom with equal velocities.

Such a flux can be characterized by a mean target density $\langle \Re \rangle$ is the in Atoms/cm^3 which can be estimated as

$$\langle \Re \rangle = \frac{\frac{4}{3}\pi r_p^3}{\pi r_f^2 \langle h \rangle} \Re \tag{4}$$

$\langle h \rangle$ is the mean distance between pellets in the vertical direction (the density is reduced by a factor equals to the volume of the pellet divided by volume of the cylinder where the pellet is located).

The dependence of the flux mean thickness on horizontal co-ordinate of an antiproton in the case of cylindrical flux and uniform distribution of the pellets inside it can be written as:

$$\rho_{mean}(x) = \langle \Re \rangle \begin{cases} 2\sqrt{r_f^2 - x^2} & if \quad |x| < r_f \\ 0 \quad if & |x| \geq r_f \end{cases} \tag{5}$$

where r_f is the pellet flux radius. (The mean thickness does not depends on the beam vertical size.) The target effective thickness can be estimated as averaging of this value over the ion distribution:

$$\rho_{eff,mean} = \int \rho_{mean}(x) f(x) dx, \tag{6}$$

where $f(x)$ is the ion distribution over the horizontal co-ordinate. For Gaussian distribution of the antiprotons the mean effective thickness is

$$\rho_{eff,mean} = \frac{\langle \Re \rangle}{\sqrt{2\pi}\sigma_x} \int_{-r_f}^{r_f} 2\sqrt{r_f^2 - x^2} \exp\left(-\frac{x^2}{2\sigma_x^2}\right) dx. \tag{7}$$

The ratio between maximum (3) and mean (7) effective target thickness is a function of the antiproton beam rms dimensions and it can be used as a criterion for choice of optimum beam emittance for the experiment. For instance a pellet target at parameters listed in the Table 1 provides the mean target thickness over $4 \cdot 10^{15}$ atoms/cm^2 (which is necessary for PANDA experiment) at the horizontal beam size below 1 mm (Fig. 1).

Table 1. Typical parameters of the pellet target

Frozen hydrogen density	Atoms/cm^3	$4.26 \cdot 10^{22}$
The pellet radius	μm	15
The pellet flux radius	mm	1.5
Mean distance between pellets	mm	5
Mean target density	Atoms/cm^3	$1.7 \cdot 10^{16}$

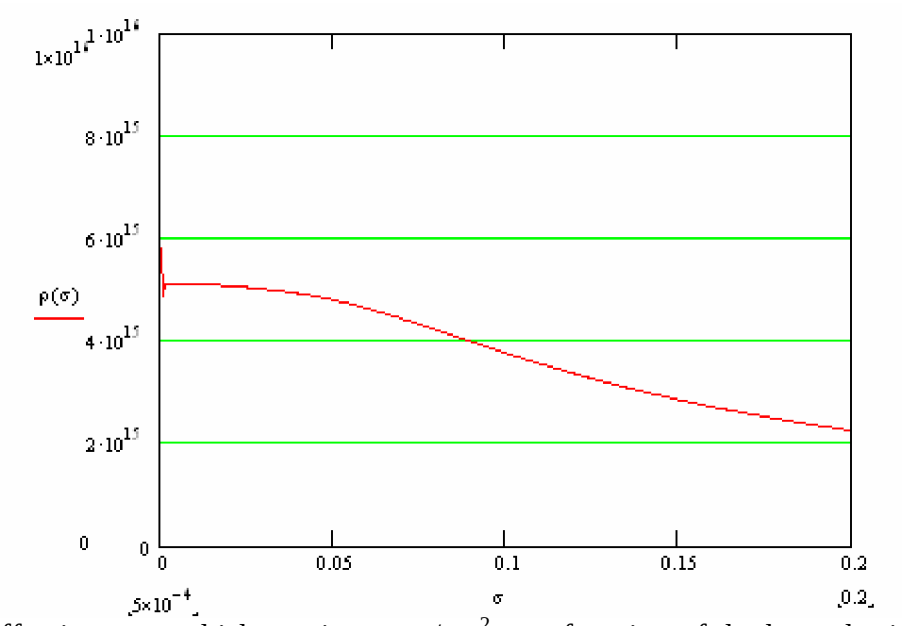

Fig. 1. Mean effective target thickness in atoms/cm^2 as a function of the beam horizontal rms size (in cm). Calculated for Gaussian distribution (formula 7).

For a round beam (if $\sigma_x = \sigma_y$) the ratio between maximum and mean effective density is shown in the Fig. 2. At the beam size of 1 mm the ratio is equal to about 2 and increases with decrease of the beam size. At the beam size of 0.5 mm the ratio reaches the value of about 8. Thus, limiting the maximum acceptable ratio by the value, for instance, 5 one can conclude that the optimum beam size lies between 0.6 and 1 mm.

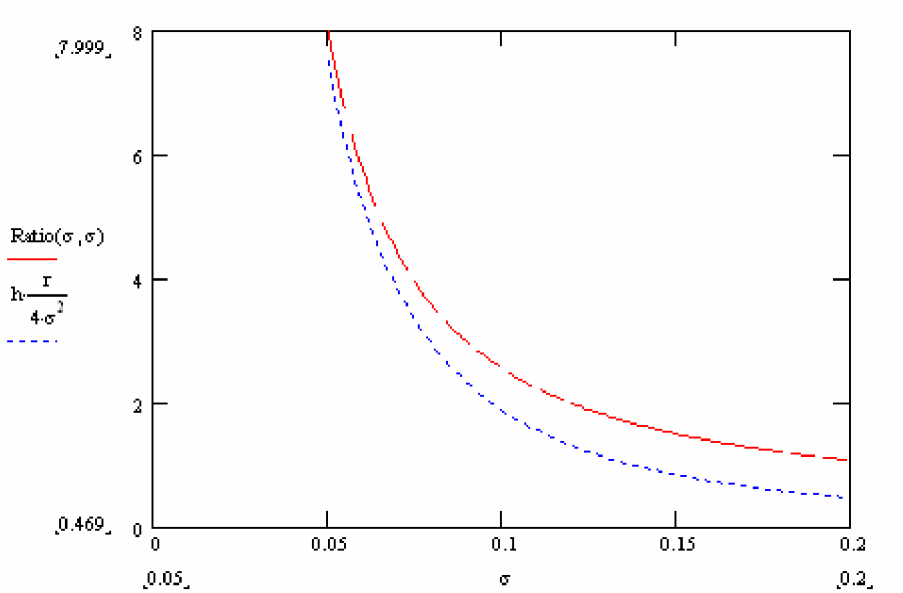

Fig. 2. Ratio between maximum and mean effective density as a function of rms beam size (in cm). Gaussian distribution.

Analytical estimation

In order to make the thinking a little easier, we will assume the pellets to be little cylinders, which are hit by the antiproton beam on a side:

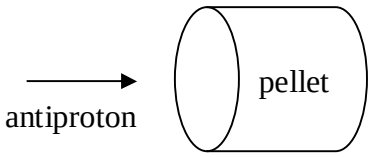

It will turn out, that the shape of the pellet will vanish from the calculation. The cylindrical pellets have the length l and radius r_p. As before, we suppose the vertical separation between pellets to be $\langle h \rangle$ and the radius of the pellet stream to be r_f. For the round antiproton beam, when $\sigma_x = \sigma_y = \sigma$, the distribution of antiprotons is

$$\rho = \frac{N_b}{2\pi\sigma^2}\exp\left(-\frac{r^2}{2\sigma^2}\right),$$

where $r^2 = x^2 + y^2$ and N_b is the number of antiprotons. The luminosity has a maximum value when the pellet is located in the centre of the beam and the number of antiproton, which hit the pellet in this case, is $\int_0^{r_p} \rho\, 2\pi r dr$. Suppose the number of hydrogen atoms containing in one pellet to be N_p, the pellet density can be written as $\Re = \frac{N_p}{\pi r_p^2 l}$. The instantaneous luminosity at pellet position in the beam center is

$$L_{\max} = \int_0^{r_p} \rho \cdot 2\pi r dr \cdot \frac{N_p}{\pi r_p^2 l} l \cdot f_{rev}$$

where f_{rev} is the beam revolution frequency. Calculation of the integral gives

$$L_{\max} = N_b\left(1-\exp\left(-\frac{r_p^2}{2\sigma^2}\right)\right)\cdot\frac{N_p}{\pi r_p^2} f_{rev}$$

Assuming $r_p << \sigma$ this expression can be rewritten in the following form

$$L_{\max} = \frac{N_b N_p f_{rev}}{2\pi\sigma^2}$$

where the dependence on the pellet dimensions disappears.

The mean luminosity, in a beam which is small compared to r_f , and travels along a diameter of the pellet stream, is

$$\langle L \rangle = N_b \frac{N_b}{\langle h \rangle \pi r_f^2} \cdot 2r_f \cdot f_{rev}.$$

The ratio of peak to mean luminosity in this case is

$$\frac{L_{\max}}{\langle L \rangle} \approx \frac{\langle h \rangle r_f}{4\sigma^2},$$

and this approximated formula (shown in the Fig. 2 with a blue line) can be used at beam dimensions less than the flux radius by larger than the pellet radius.

More accurate treatment of two dimensional case, given in V.Zeemann, On pellet target luminosity modulation, TSL, Uppsala University, 2005, at analogous approximation leads to

$$\frac{L_{\max}}{\langle L \rangle} \approx \frac{\langle h \rangle r_f}{2\sqrt{\pi}\sigma_x\sigma_y}.$$

For the round beam that practically coincides with the previous formula. As one can see from the Fig. 2 these estimations are in good agreement with more accurate calculations, when the beam size is two times less than the pellet stream radius.

2. Emittance control by electron beam misalignment

2.1. Hopf bifurcation and chromatic instability

The antiproton angular spread corresponding to the beam emittance of about of 10^{-7} π·m·rad is equal to $\sqrt{\varepsilon / \beta_{CS}}$, where β_{CS} is the beta function in the cooling section. At β_{CS} of about 100 m the angular spread is about 30 μrad. Misalignment of the electron beam can be used for stabilization of the emittance value. However, at small angles the misalignment leads to decrease of the cooling efficiency only, but the beam emittance is determined by equilibrium between cooling and heating (due to interaction with the target and intrabeam scattering). When the misalignment reaches a certain threshold value a qualitatively different situation is obtained. The ions starts to oscillate with a certain value of betatron amplitude. The amplitude of the oscillations depends on misalignment angle and the beam emittance (independently on additional heating) can not be less than the value corresponding to oscillation amplitude. In absence of another effects leading to heating of the beam, the beam profile has specific double-peak structure, and sudden appearance of this structure at variation of misalignment angle is called “chromatic instability”.

The appearance of betatron oscillations is caused by a non-linear friction force acting on an ion moving inside electron beam. The force has a maximum at certain relative velocity and the threshold of chromatic instability is located where the transverse velocity component of the misaligned electron beam is equal to the velocity of the force maximum.

This transition from stable particle motion, described by a stable fixed point in the phase space, to oscillating motion corresponding to a circular attractor, or limit cycle, is known as a Hopf bifurcation. Estimation of the amplitude of oscillations can be done for simplified shape of the friction force. At small ion velocity the friction force is almost linear with relative velocity, in the large velocity range the friction force decreases as $1/v^2$. Combination of these asymptotes leads to the friction force shape shown in the Fig. 3. Here the friction force is normalized on its maximum value, the velocity is measured in units of that one corresponding to the maximum position.

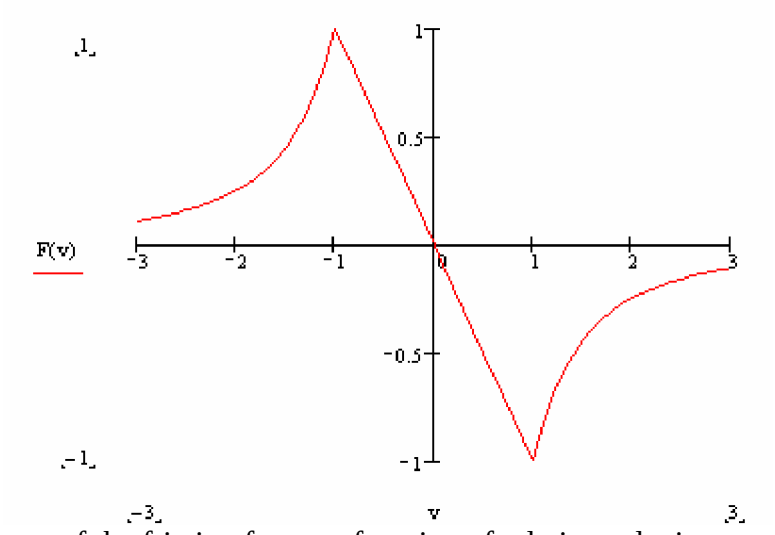

Fig. 3. Simplified shape of the friction force as function of relative velocity.

A change of the energy of ion transverse motion during one betatron oscillation can be written as

$$\Delta E = \int_0^{2\pi} F_\perp(v_\perp) v_\perp d\varphi \ , \qquad (8)$$

where φ is the phase of oscillations. At the attractor the particle motion satisfies the condition $\Delta E = 0$. If the particle velocity oscillates with a certain amplitude V_{max} and there is transverse electron velocity of V_{shift} due to misalignment, the amplitude of oscillations corresponding to motion at attractor can be found from the equation:

$$\int_0^{2\pi} F\left(V_{\max}\cos\varphi - V_{shift}\right)\cos\varphi d\varphi = 0\,. \tag{9}$$

Dependence of integral (9) on amplitude of the oscillations at different misalignments is shown in the Fig. 4. When the electron velocity shift is less than maximum position the energy gain is negative for all amplitudes of oscillation. It means that the particle is cooled down to zero amplitude.

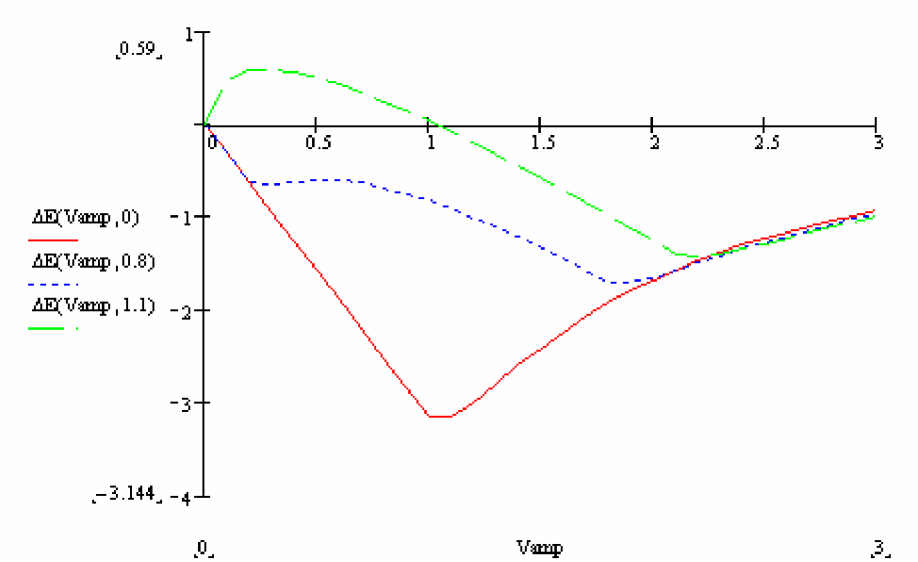

Fig. 4. Energy gain at one betatron oscillation as a function of amplitude. Red curve – electron and ion beam are perfectly aligned, blue curve – the angle is equal 0.8 of the threshold value, yellow line – the angle is 1.1 of the threshold value.

When the velocity shift is larger than the maximum position the energy gain at small amplitudes is positive. The condition (9) is satisfied at zero amplitude and at certain value. Zero amplitude corresponds to unstable equilibrium point, and small inclination of the ion velocity from zero value leads to increase of the amplitude to the value corresponding to the attractor. In the Fig. 5 the amplitude of oscillations corresponding to the attractor is shown as a function of the electron velocity shift.

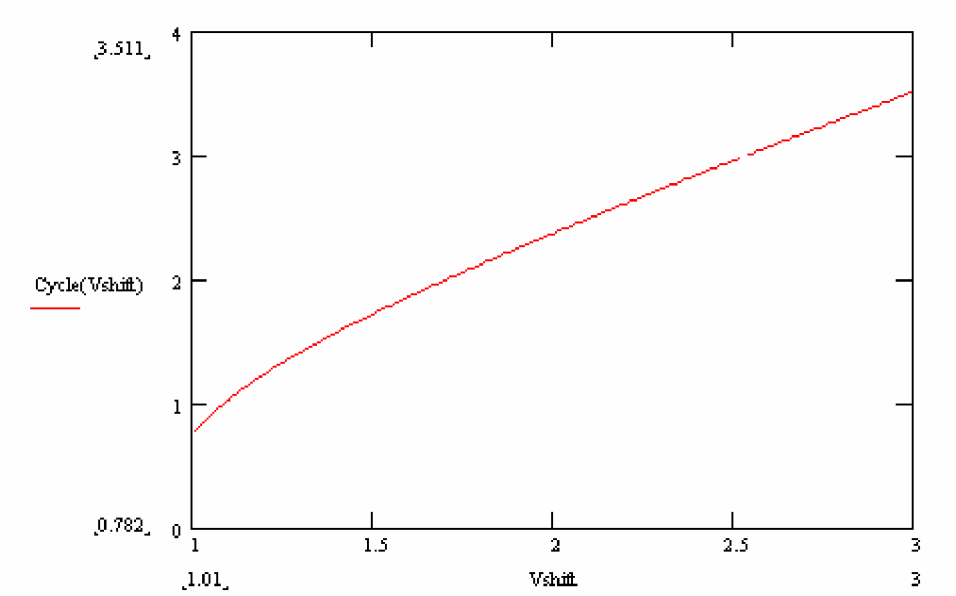

Fig. 5. Oscillation amplitude at the attractor as a function of velocity shift.

When the velocity shift is larger than maximum position by about 1.5 times, the amplitude of oscillations is practically linearly proportional to the velocity shift: $V_{max} \approx 1.2V_{shift}$. If all the particles ascillate with the same amplitude the rms velocity spread in the beam can be calculated as

$$V_{rms}^2 = \frac{1}{2\pi}\int_0^{2\pi} V_{\max}^2 \cos^2\varphi d\varphi = \frac{V_{\max}^2}{2}.$$

The rms velocity spread within an accuracy of 20% is equal to the velocity shift. Correspondingly, to stabilize the beam emittance at the value of ε one needs to introduce an angle of about

$$\theta_{shift} = \frac{V_{shift}}{\beta\gamma c} \approx \sqrt{\frac{\varepsilon}{\beta_{CS}}}.$$

At magnetized cooling velocity corresponding to the force maximum is determined by temperature of longitudinal degree of freedom of electrons. In high voltage cooling system the longitudinal temperature is determined mainly by HV ripple. Design value of relative HV ripple at HESR cooling system is equal to $(2\div3)\cdot10^{-5}$ that corresponds to longitudinal temperature below 0.5 meV. The rms electron velocity spread determining the position of friction maximum is equal

$$V_{\|,rms} = \beta c\frac{\Delta p}{p} = \beta c\frac{\gamma}{\gamma+1}\frac{\Delta U}{U},$$

and misalignment angle corresponding to the threshold of the chromatic instability is approximately equal to

$$\theta_{th} \approx \frac{V_{\|,rms}}{\beta\gamma c} \approx 3\mu rad.$$

Position of the friction force maximum can be displaced into region of larger velocity due to errors of the magnetic field in the cooling section. Any case one can expect (and it is our goal if we want to stabilize the emmitance) Hopf bifurcation of the stable antiproton trajectory, and as a result development of chromatic instability.

2.1. Luminosity variation at chromatic instability

If the misalignment angle is larger than the threshold of chromatic instability and intrabeam scattering is negligible, all the antiprotons oscillate with the same amplitude of betatron oscillations. The mean effective target thickness calculated for a particle at some amplitude of horizontal betatron oscillations A is equal to:

$$\rho_{single,mean} = \frac{1}{2\pi}\int_0^{2\pi} \rho_{mean}(A\cos\varphi)d\varphi\,, \tag{10}$$

and rms beam size relates to the amplitude as:

$$\sigma = \frac{A}{\sqrt{2}}\,. \tag{11}$$

In this case the mean effective thickness depends on the beam size similarly to the case of Gaussian distribution until the amplitude of the oscillations is less than the flux radius (Fig. 6). When the amplitude begins to be large than the flux radius the thickness drops down fast. Therefore the choice of rms beam size is limited by the value $\sigma \leq 1$ mm.

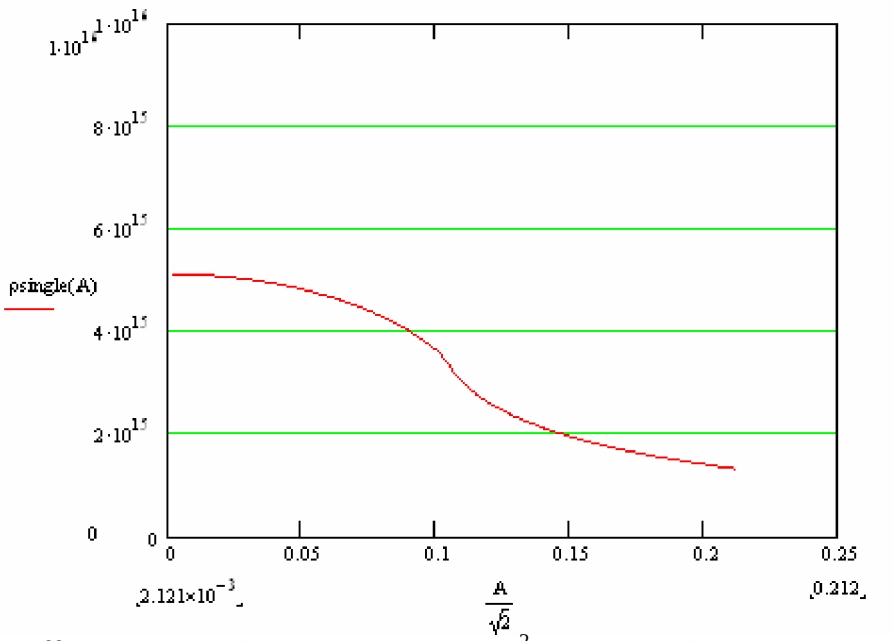

Fig. 6. The mean effective target thickness in atoms/cm^2 versus rms beam size in cm when all the antiprotons have the same amplitude of betatron oscillations.

The beam profile has a specific shape with dept in the central part (hollow beam) and maximum effective thickness corresponds to situation when the pellet is located at the edge of the beam. The ratio between maximum and mean luminosity can be simply estimated for one-dimensional betatron oscillation. Lower estimation can be done assuming uniform antiproton distribution in the vertical direction. In this case the target effective thickness as a function of the pellet horizontal position X can be calculated as:

$$\rho_{\sin gle,\max} = \frac{2r_p}{\langle h \rangle} \Re \frac{2}{2\pi} \int_{\arcsin\left(\frac{X-r_p}{A}\right)}^{\arcsin\left(\frac{X+r_p}{A}\right)} 2\sqrt{r_p^2 - (A\sin\varphi - X)^2}\, d\varphi \ . \qquad (12)$$

The multiplier 2 before the integral appeared because the antiproton crosses the pellet two times during one period of betatron oscillations.

The target thickness when the pellet is located in the centre of the beam is equal to about $4 \cdot 10^{15}$ atoms/cm^2 (rms beam size is 1 mm). At the pellet location at the edge of the beam this value exceeds $2 \cdot 10^{16}$ atoms/cm^2 (Fig. 7).

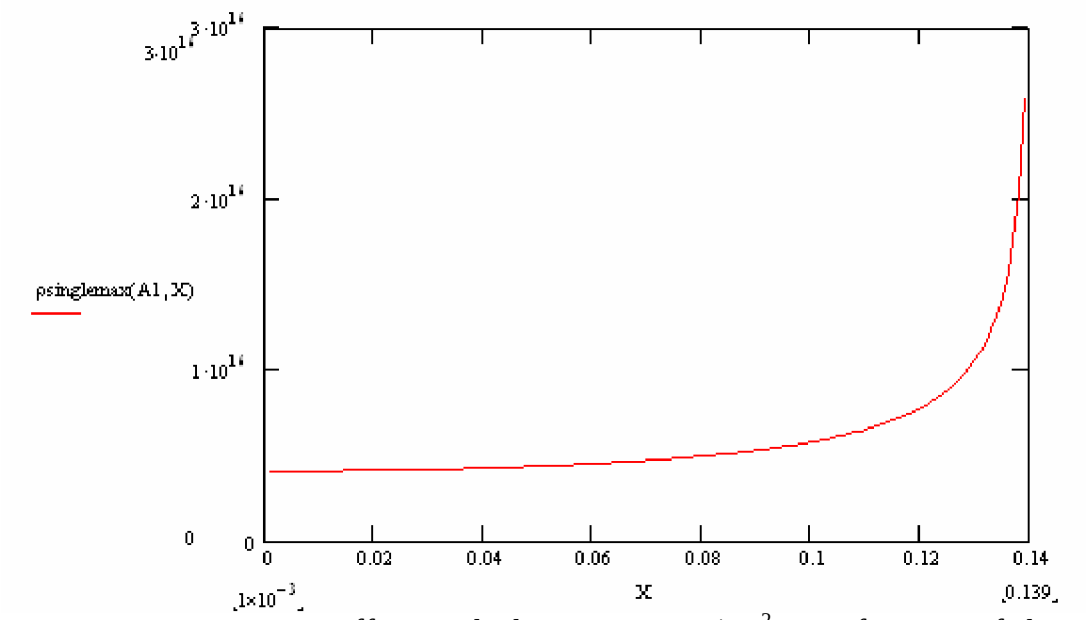

Fig. 7. Maximum target effective thickness in atoms/cm^2 as a function of the pellet horizontal position in cm. The amplitude of the horizontal oscillations is 1.41 mm (rms beam size is 1 mm).

The ratio between maximum and mean luminosity has a minimum at the beam size in the range from 0.2 and 1 mm which is approximately equal to 10 (Fig. 8).

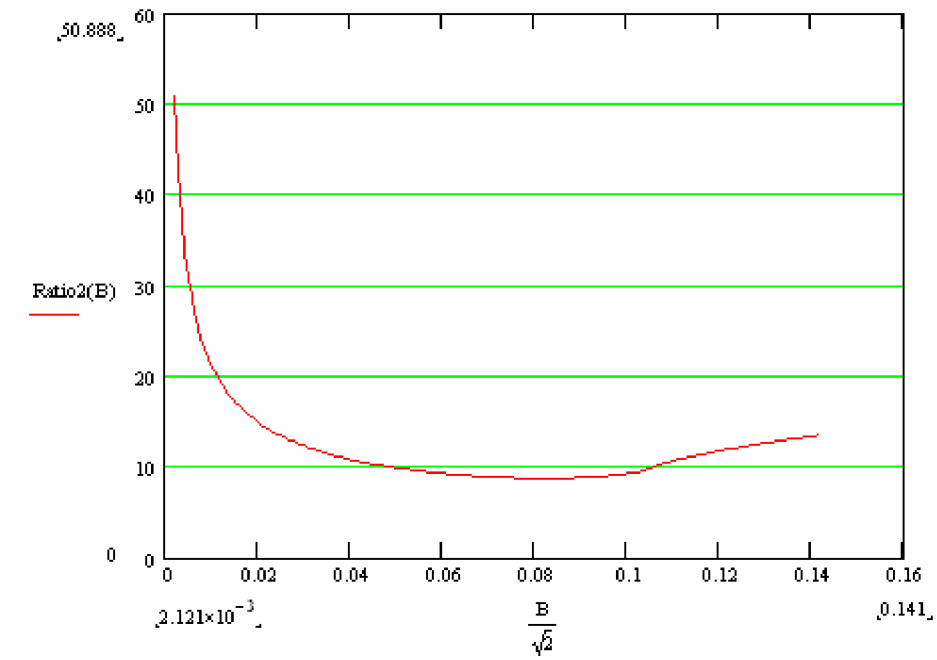

Fig. 8. Ratio between maximum and mean effective density as a function of rms beam size (in cm). One-dimensional horizontal oscillations, uniform distribution in the vertical dimension.

In the case of two dimensional oscillations the situation is even worth. Therefore to keep the ratio between maximum and mean luminosity in the required range one needs to avoid formation of the double peak structure of the beam profile.

2.2. Beam profile at cooling with misaligned electron beam

One of the effects which can suppress development of chromatic instability is intrabeam scattering in the ion beam. For instance, the dependence of the proton beam profile on misalignment angle was investigated at S-LSR (Kyoto university) during February - March of 2007 at parameters listed in the Table 2. The transverse profiles were measured by the ionization monitors with various misalignment angles (Fig. 9, 10). The particle number was large enough: 1×10^7 at the electron current of 25.5 mA and 3×10^7 at 102 mA.

Table 2. S-LSR experimental parameters

Proton Energy	7 MeV
Revolution Frequency	1.61 MHz
Electron Current	25.5 mA or 102 mA
Electron Beam Radius	25 mm
Magnetic Field of Solenoid	500 Gauss

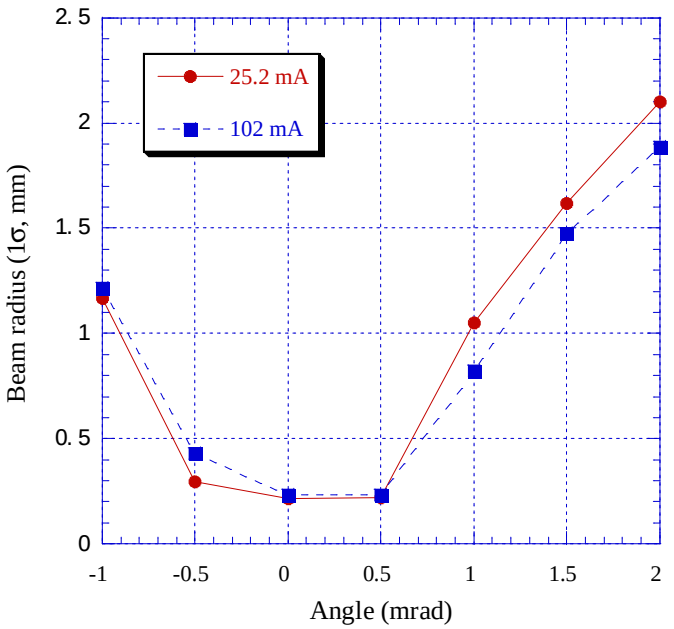

Fig. 9. Transverse beam radius as a function of the horizontal misalignment angles with two different electron currents. The particle number was 1×10^7 (25.2 mA) and 3×10^7 (102 mA). S-LSR.

The profile width has almost constant value when the angle is close to zero and increase very fast with increase of the angle starting from some threshold value (Fig. 9). Simulations with Betacool program with these parameters indicate development of chromatic instability. The beam profile has a well pronounced double peak structure and most of the particles oscillate with the same amplitude in the horizontal plane (Fig. 11). (The amplitude of oscillation at limit cycle is almost equal to misalignment angle as it follows from simplified model of the friction force described in the chapter

2.1) In the simulation an analytical model of IBS developed for a beam with Gaussian distribution was used.

However, the measured beam profiles have practically Gaussian shape up to very large misalignment angle (Fig. 10). It can be explained by peculiarities of IBS process, which were not taking into account in simulations. More probably IBS leads to very fast relaxation of the distribution function to equilibrium Gaussian shape. This hypothesis is approved by dependence of the profile on the particle number in the ring.

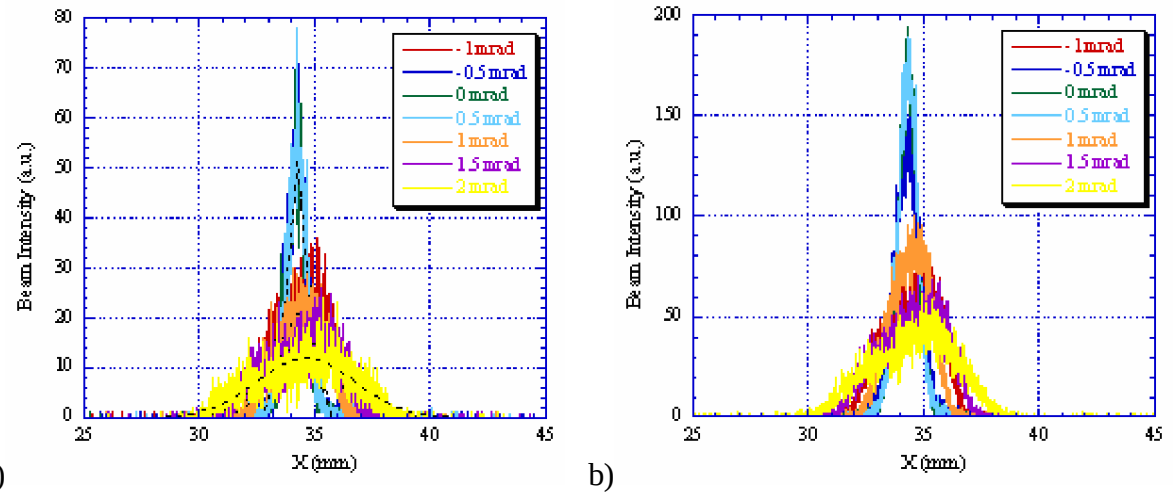

a) b)

Fig.10. Transverse beam profiles measured by the ionization monitors. The electron current was 25.5 mA (a) and 102 mA (b). Horizontal misalignment angles -1, -0.5, 0, 0.5, 1, 1.5, 2 mrad. S-LSR.

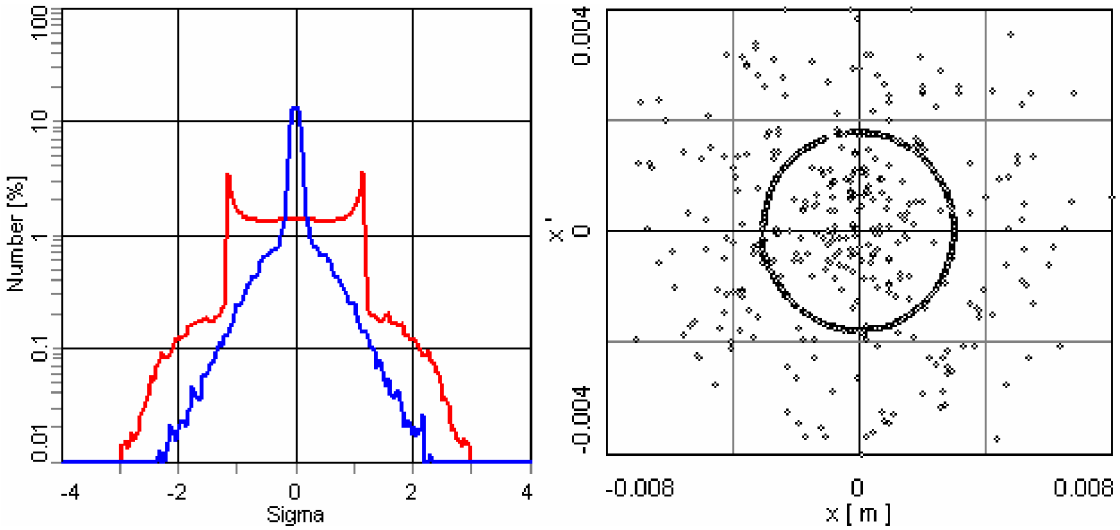

Fig.11. Simulation with Betacool of transverse profiles (red curve in the left plot corresponds to horizontal profile, blue one – to vertical) and the particle distribution in the horizontal phase space (right plot) for N_p=3×10^7, I_e=100mA and horizontal misalignment 2 mrad. S-LSR.

The profile width does not depend on the particle number practically (right plot in the Fig. 12). And only at extremely small particle number the profile has a double peak structure (left plot in the Fig. 12).

It should be noted that the electron beam misalignment provides required transformation of six dimensional phase volume independently on development of chromatic instability. In the Fig. 13 the momentum spread of the proton beam as a function of the particle number is shown. At all

intensities the misalignment leads to decrease of the beam momentum spread by 1.5 – 2 times, and this effect is more pronounced at small electron current.

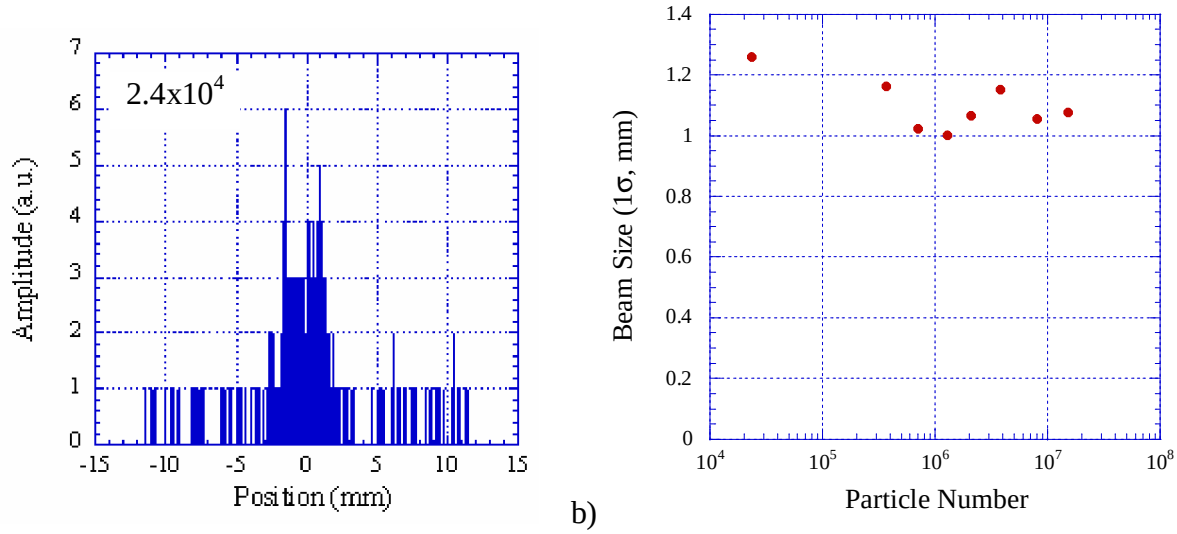

a) b)

Fig.12. Transverse beam profile with the horizontal misalignment of 1mrad (a) for Np=2.4×10^4 and transverse size as a function of the particle number (b). S-LSR.

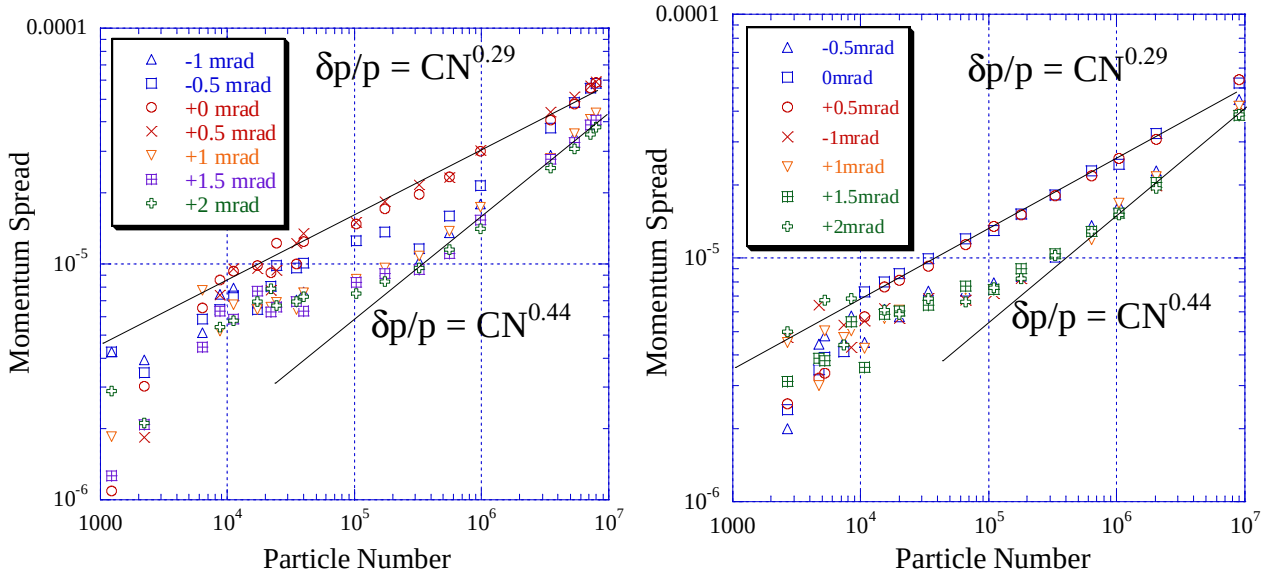

Fig.13. Momentum spread as a function of particle number with seven kinds of horizontal misalignment angle. The electron current is 25.5 mA (left) and 102 mA (right). S-LSR.

Another possible mechanism of the chromatic instability suppression is errors of the magnetic field. For instance, measurements of the proton beam profile width as a function of misalignment angle are used at COSY for optimization of the cooler settings. The experiments are provided at injection energy of 45 MeV. The beam profiles in the cooling section are measured with the neutral-particle (H^0) profile detector. The measurements are performing at relatively large proton number – $10^9 \div 10^{10}$ (that corresponds to better sensitivity). A double peak structure of the profiles was never observed in such a measurements, that can be explained by chromatic instability suppression due to powerful IBS process.

The results of November 2001 shown in Fig. 14 demonstrates that in the horizontal plane the H^0 width is extremely sensitive to small angle variations, whereas the dependence in the vertical plane is flat, at least within ± 0.4 mrad. Minimum of the horizontal profile width corresponds to some non zero inclination angle between the electron beam and the proton orbit.

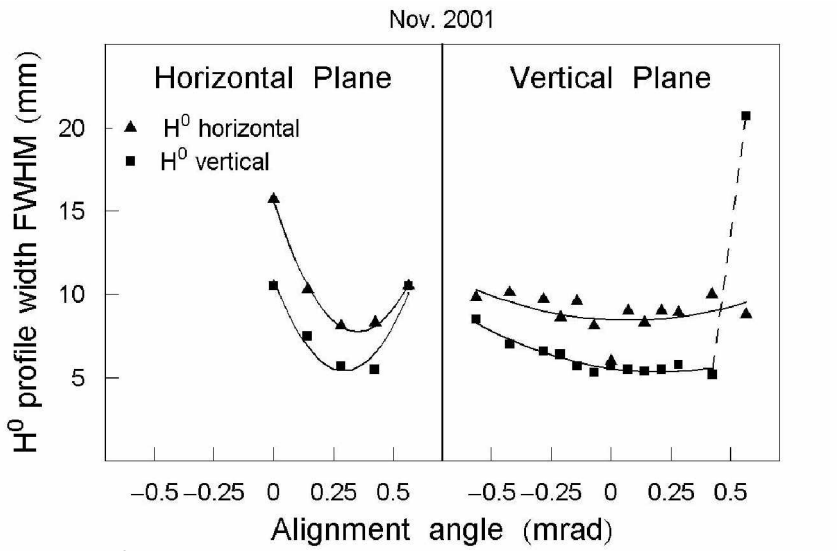

Fig. 14. Dependence of the H^0 width on the alignment of the e beam. For the vertical plane the horizontal setting was + 0.35 mrad. COSY.

The H^0 profile width can be recalculated into the profile width in the cooling section (the monitor is located by about 25 m downstream the cooling section). The vertical beam profile width in the cooling section always by about two times larger than the horizontal one (Fig. 15). It is partially explained by difference in beta functions – the horizontal one is about 7 m, the vertical – about 17 m. However, the measured profiles correspond to the vertical emittance larger than the horizontal one. Intrabeam scattering simulations predict opposite situation: as in most of storage rings the horizontal heating rate at COSY lattice is larger than the vertical one.

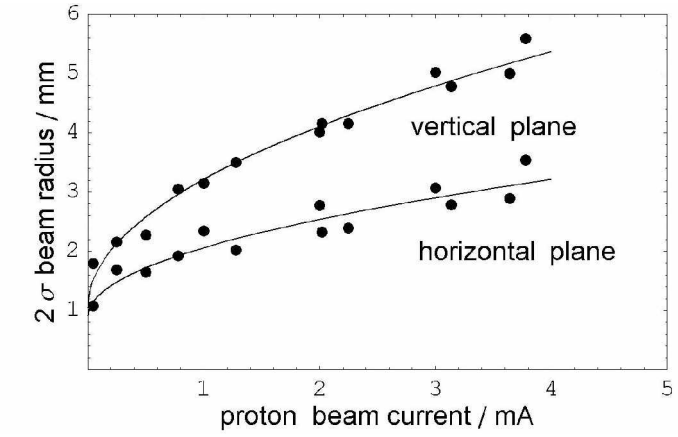

Fig 15. Beam radius in the cooling section as a function of the proton number at best alignment of the electron beam. The data from June and September of 2004. COSY.

Such a different behavior of the profiles in horizontal and vertical plane can be explained on the basis of magnetic field geometry in the cooling section (Fig. 16). The magnetic fields in the cooling section were measured during the cooler commissioning in 1992 using the "magnetic mirror" technique. It had been applied to measure the straightness of the magnetic field lines in the drift solenoid in the range from 0.08 to 0.15 T. Lower fields than 0.08 T are not applicable due to the limited range of control of the gun and drift solenoid shunts. In Fig. 12 (a) and Fig. 12 (b) are shown the horizontal and vertical field line angles along the axis of the cooling section solenoid as it was manufactured (the solenoid length is 2 m). After appropriate correction the field line inclinations were reduced to the value of below $2 \cdot 10^{-4}$ in both planes. However up to 2006 all electron cooling applications were run with the uncorrected 0.08 T field. Correspondingly all the measurements of the profile width were performed with uncorrected fields.

From the Fig. 12 (a) one can see that introducing some regular angle of about $+2 \cdot 10^{-4}$ the horizontal angles of the magnetic field can be localized in the range of $\pm 2 \cdot 10^{-4}$ at the length of about 1.5 m (this value is usually used as an "effective length" of the cooler solenoid for the friction force evaluation at COSY). In the vertical plane the angle between field line and the solenoid axis varies from $-1 \cdot 10^{-3}$ to $+1 \cdot 10^{-3}$ along the cooler. The region where the angles lie in the range of $\pm 2 \cdot 10^{-4}$ is less than 1 m. And this length varies insufficiently at introducing of a regular angle.

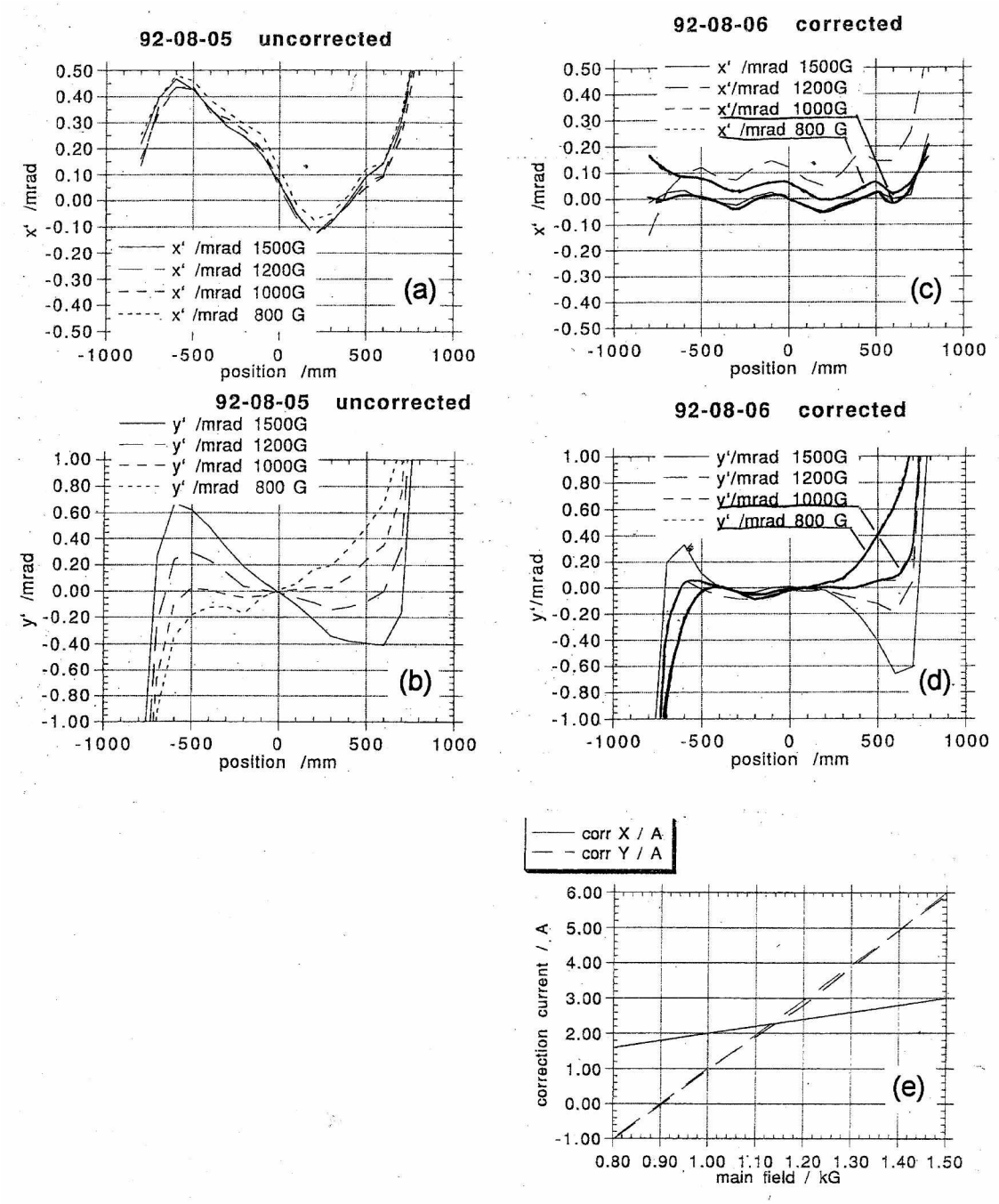

FIG. 16. Measurements of the magnetic field line angles along the drift solenoid. (a) and (b) the horizontal (x) and vertical (y) field angles of the solenoid as it was manufactured, (c) and (d) after appropriate correction using saddle coils with varying azimuthal angle, (e) the saddle coil currents to be applied for different longitudinal field values.

2.3. Chromatic instability in presence of a pellet target

In the case of beam misalignment using for emittance stabilization at HESR one can not hope for the chromatic instability suppression by intrabeam scattering, because the goal of the misalignment is to decrease the IBS heating rates to negligible level. Requirements to the magnetic field accuracy in the cooling section are also very strong. Therefore only the process which can suppress the instability is the interaction with the pellet target. The antiproton scattering with the pellet target leads to diffusion in the transverse phase plane. In the case of chromatic instability this diffusion will lead to formation in the transverse plane a cycle of a finite thickness filled with the particles. Thickness of the cycle is determined by ratio between cooling power provided by electron beam and heating power from the target (in absence of additional heating the ion distribution over amplitude of oscillations is delta-function). By optimization of electron beam current value one can try provide a thickness of the cycle required for minimization of maximum to mean luminosity ratio. The electron current is limited from the lower side by requirement to stabilize the tails of distribution function.

To estimate achievable equilibrium beam parameters the antiproton dynamics was studied with Betacool program using Model Beam algorithm. For compensation of mean energy loss in the target RF voltage of 1 V at the first harmonic of revolution frequency was applied. At the momentum spread of 10^{-5} it corresponds to rms bunch length of about 40 m, that is sufficiently less than the ring circumference (as it will be shown latter this voltage is not big enough at interaction with internal target and some particle loss from the separatrix took a place).

Assuming that the beta-functions in the target position are 8 m in both planes, the equilibrium emittance was chosen to be $4\cdot10^{-8}$ $\pi\cdot$m$\cdot$rad. This value corresponds to rms beam transverse size of 0.6 mm which is close to optimum value. The antiproton beam rms size in the cooling section is 2 mm if the beta-function in the cooling section is 100 m. At electron beam radius of 5 mm more than 90% of antiprotons cross the cooling section inside the electron beam. To provide such an emittance the electron beam misalignment angle has to be about $2\cdot10^{-5}$. At zero initial position of the electron beam in the cooling section its final co-ordinates have to be equal to about 0.5 mm.

All other parameters of the electron cooling system were chosen to be close to HESR design values. The electron transverse temperature was chosen to be close to the maximum value at the edge of the electron beam. For the friction force calculation the semi empirical formula by Parkhomchuk was used. It gives relatively conservative estimation and takes into account the magnetic field errors as a part of effective temperature. At the field accuracy from the Table 3 the effective temperature is about 1.5 meV and dominated by the field errors.

Table 3. General parameters of electron cooling system used in simulations

Cooling section length	m	24
Electron beam radius	mm	5
Magnetic field in the cooling section	kG	2
Relative errors of the magnetic field		$5\cdot10^{-6}$
Maximum electron current	A	1
Transverse electron temperature	eV	1
Longitudinal electron temperature	meV	0.5
Electron beam co-ordinates at the entrance of the cooling section (horizontal/vertical)	mm	0/0
Beta-functions in the cooling section (horizontal/vertical)	m	100/100
Electron beam co-ordinates at the entrance of the cooling section (horizontal/vertical)	mm	0.5/0.5

The number of modeling particles was 8000, that is large enough to provide analysis of the distribution shape in its central part (for simulations of the tails of distribution function the particle number has to be at least one order magnitude larger). Integration step over time was chosen to be 0.1 sec. At larger value electron cooling efficiency can be underestimated in the central part of the beam.

Initially simulations were performed in absence of the internal target. Intrabeam scattering was simulated using Martini model and diffusion power was equal for all particles independently of their velocities (Gaussian model). Initial values of the beam emittance and momentum spread were chosen relatively arbitrary near expected equilibrium: the initial emittance was $3 \cdot 10^{-8}$ π·m·rad, the momentum spread - $3 \cdot 10^{-5}$. At electron beam current of 0.5-1 A the time required to reach equilibrium is about 20 sec and the particle loss does not play a role at this scale. Therefore the beam intensity was supposed to be constant.

As output values for the emittance and momentum spread were chosen the square in the phase plane containing 38% of particles. For Gaussian beam this corresponds to rms emittances. The particle distribution in momentum space was close to Gaussian in all simulations and this estimation is valid within an accuracy of a few tens of percents.

Evolution of the beam emittance and momentum spread in time under the common action of electron cooling and intrabeam scattering is shown in the Fig. 17.

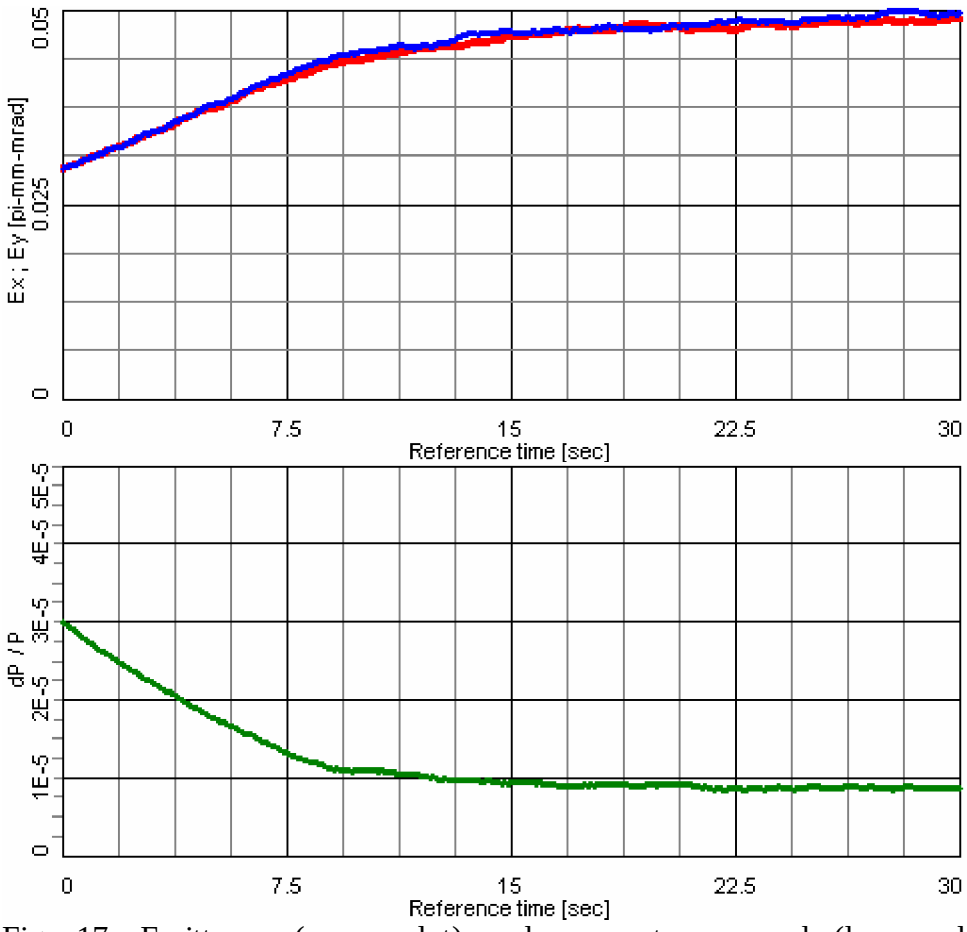

Fig. 17. Emittance (upper plot) and momentum spread (lower plot) time dependencies. ECOOL+IBS. Electron current is 1 A. HESR.

Equilibrium beam emittance is about $5 \cdot 10^{-8}$ π·m·rad that is close to expected value. The momentum spread in equilibrium lies below 10^{-5}. The particle distribution in the transverse plane after 30 sec of

the cooling has a square shape with maximum density in the corners (left plot in the Fig. 18). The particle distribution in the transverse phase planes has a shape of limit cycle at finite width (right plot in the Fig. 18).

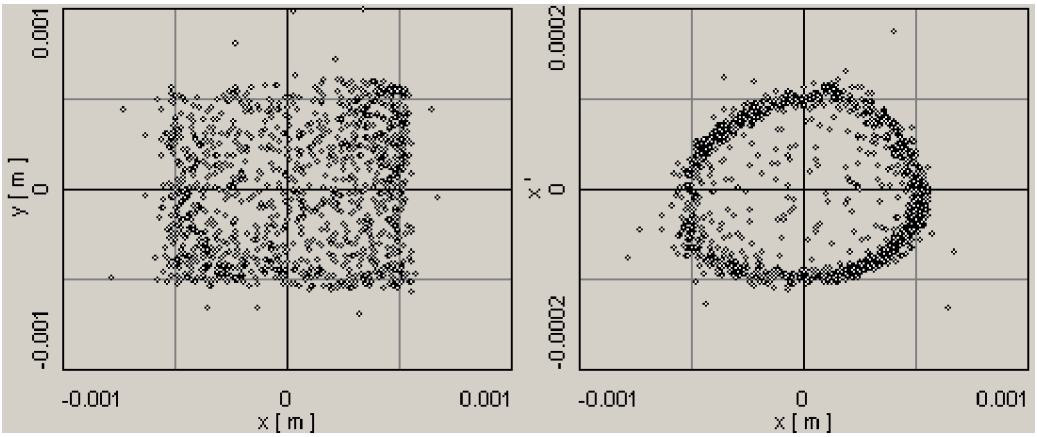

Fig. 18. Particle distribution after 30 s of cooling. ECOOL+IBS. Electron current is 1 A. HESR.

The transverse beam profiles (Fig. 19) have a shape typical for chromatic instability, but not well pronounced. Central part of the longitudinal profile can be approximated by Gaussian low with good enough accuracy.

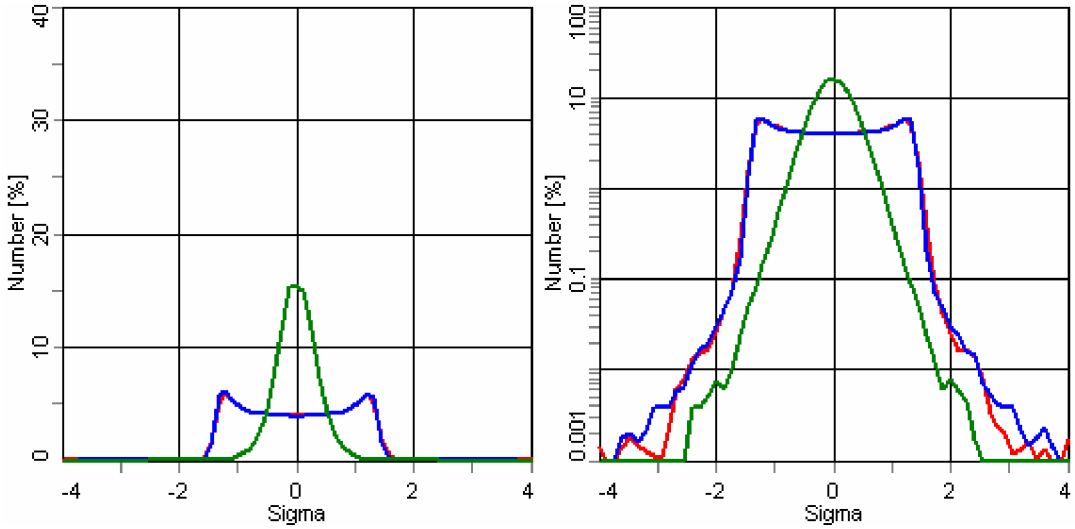

Fig. 19. Beam profiles after 30 sec of cooling in linear (left plot) and in logarithmic scales (right plot) Red line is horizontal profile, blue – vertical, green – longitudinal. Electron current is 1 A. ECOOL+IBS. HESR.

The pellet parameters in Betacool were chosen to provide required luminosity value (Table 4). In the Betacool the pellet is approximated as a rectangular box and chosen dimensions are approximately equivalent to spherical pellet at radius of 15 μm. The luminosity at such parameters was equal to about $2.15 \cdot 10^{31}$ $cm^{-2}s^{-1}$ and kept practically constant value during the simulation period.

Table 4. Parameters of the pellet target used in simulations

Frozen hydrogen density	Atoms/cm^3	$4.26 \cdot 10^{22}$
The pellet dimensions (longitudinal/horizontal/vertical)	μm	24
The pellet flux radius	mm	1.5
Mean distance between pellets	mm	4
Beta-functions in the target position (horizontal/vertical)	m	8/8

The scattering of a model particle with the pellet was simulated in accordance with Urban model for longitudinal degree of freedom (the energy loss were assumed to be only due to ionization) and as plural Coulomb scattering for transverse degrees of freedom.

The emittance and momentum spread evolution in time looks very similar to the previous case, but the final momentum spread value is less by about 3 times. It strange result will be explained from analysis of the beam profiles.

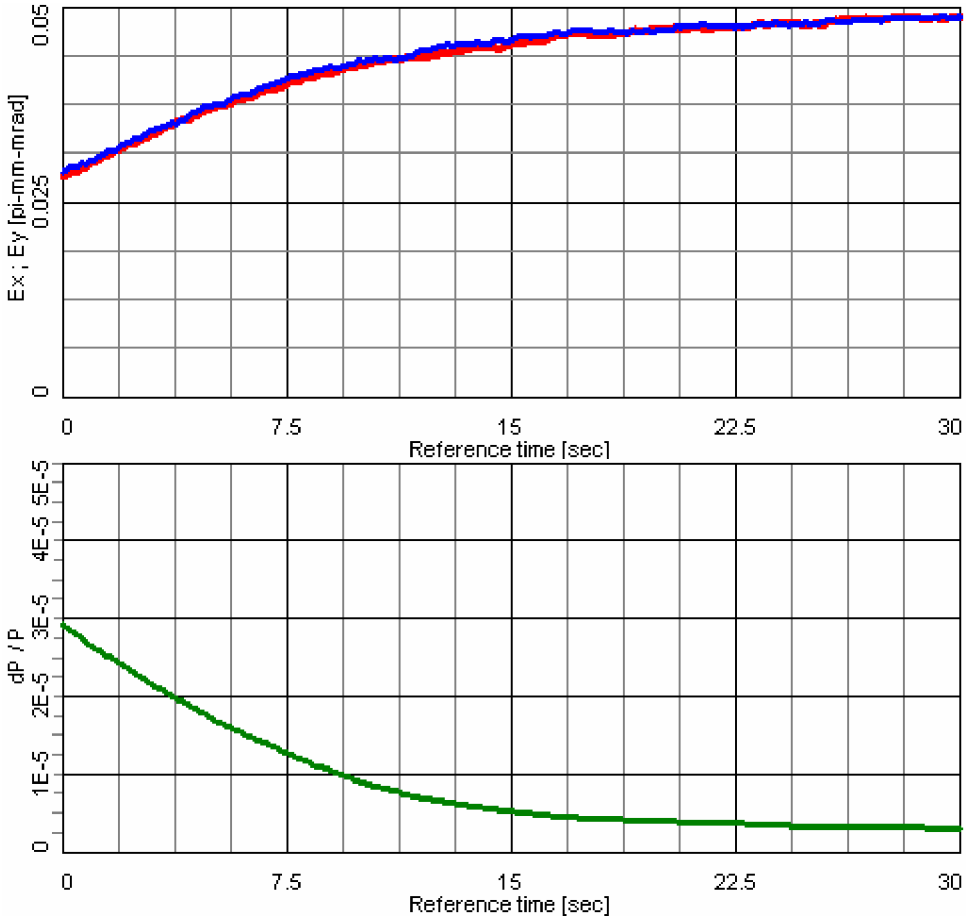

Fig. 20. Emittance (upper plot) and momentum spread (lower plot) time dependencies. ECOOL+IBS+TARGET. Electron current is 1 A. HESR.

The particle distribution in the transverse phase planes (Fig. 21, left plot) look similar to the case without the target but the edges of the limit cycle are not so sharp. It is clear from the transverse profile in logarithmic scale (Fig. 22 left plot)

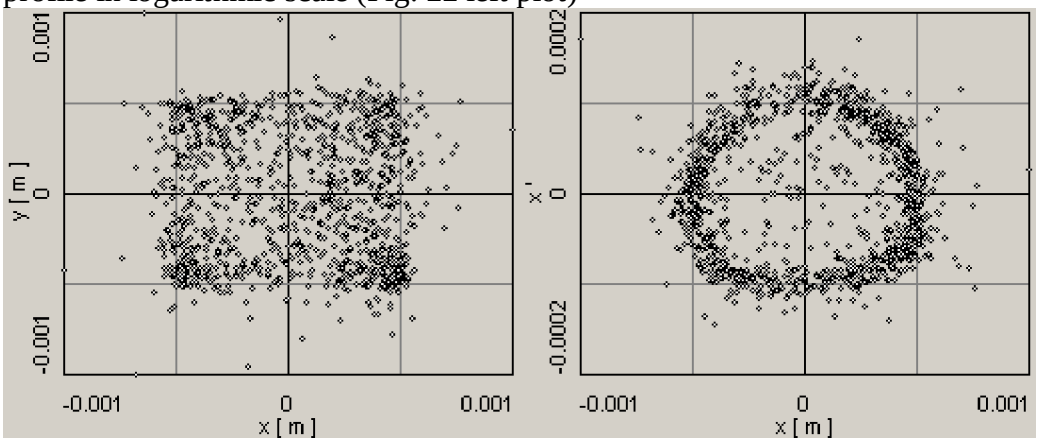

Fig. 21. Particle distribution after 30 s of cooling. ECOOL+IBS+TARGET. Electron current is 1 A. HESR.

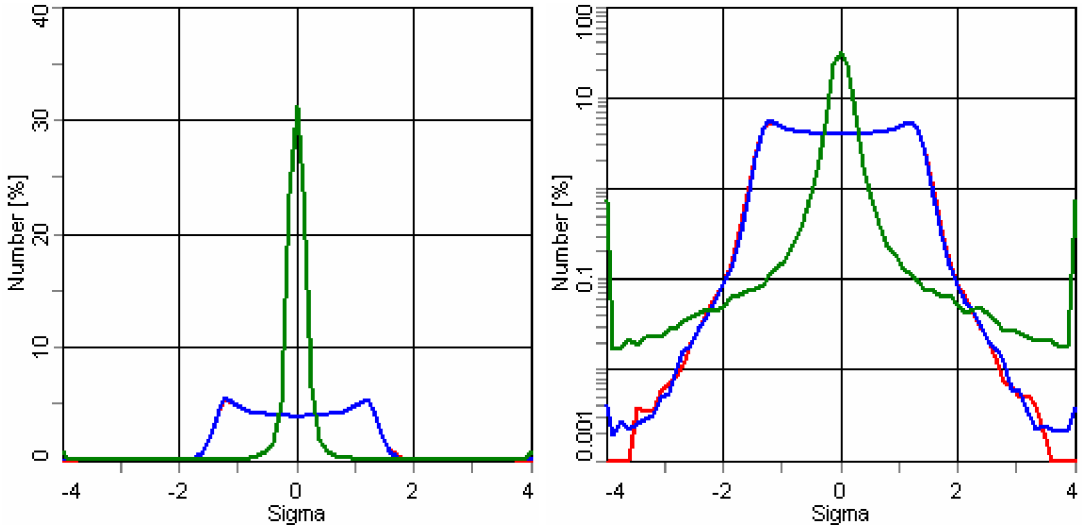

Fig. 22. Beam profiles after 30 sec of cooling in linear (left plot) and in logarithmic scales (right plot) Red line is horizontal profile, blue – vertical, green – longitudinal. Electron current is 1 A. ECOOL+IBS+TARGET. HESR.

From longitudinal profile in the logarithmic scale one can see, that the electron cooling does not suppresses formation of the tails of the distribution function due to fluctuation of the energy loss. About 1% of the particles are loosed from the bucket and form very long tails. The synchrotron motion in Betacool is simulated in the linear approximation and the real particle loss does not taking into account. For IBS diffusion power evaluation the program calculates rms parameters of the beam and formation of the long tail in the distribution function leads to artificial decrease of the diffusion. But in the transverse direction the electron cooling stabilizes the tails at reasonable values.

Decrease of the cooling power leads to further increase of the limit cycle width. At electron beam current of 0.5 A the equilibrium emittance has practically the same value as at 1 A, equilibrium momentum spread slightly increases ($5 \cdot 10^{-6}$ at 0.5 A instead of $3 \cdot 10^{-6}$ at 1 A). However the width of the limit cycle (left plot in the Fig. 23) is sufficiently larger than at 1 A, and double peak structure of the transverse profile almost disappears (Fig. 24). Instead it the profile has a wide enough edges and flat top between them.

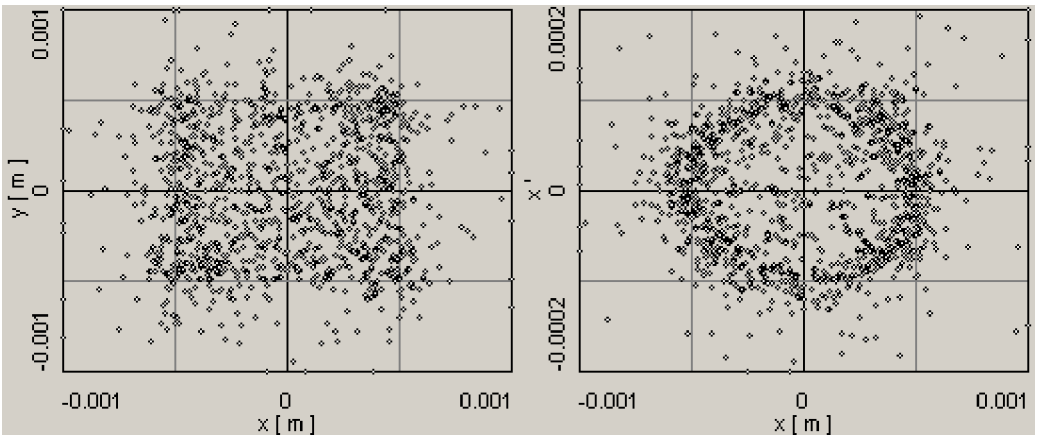

Fig. 23. Particle distribution after 30 s of cooling. ECOOL+IBS+TARGET. Electron current is 0.5 A. HESR.

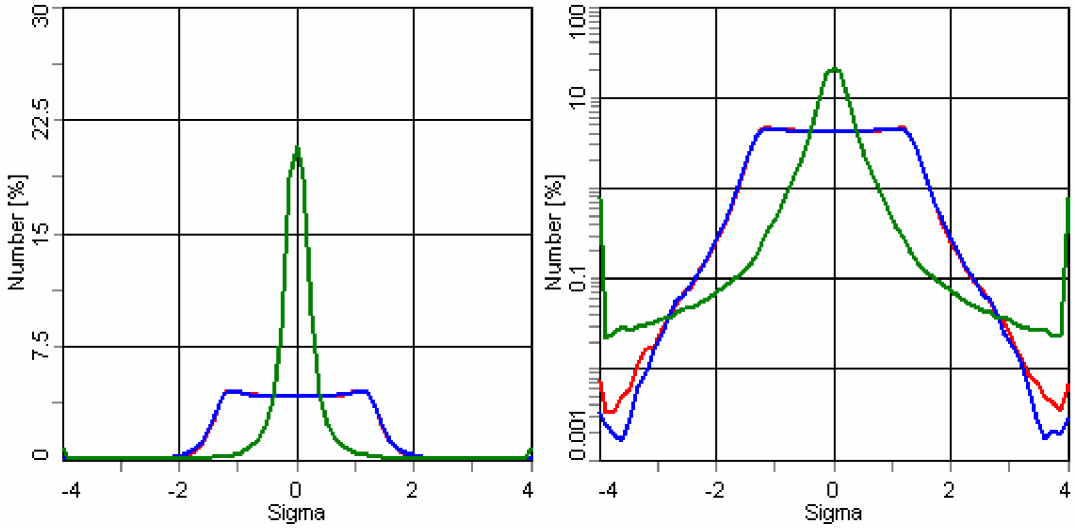

Fig. 24. Beam profiles after 30 sec of cooling in linear (left plot) and in logarithmic scales (right plot) Red line is horizontal profile, blue – vertical, green – longitudinal. Electron current is 0.5 A. ECOOL+IBS+TARGET. HESR.

The evolution of the transverse beam profile at variation of heating and cooling efficiency is obvious from the Fig. 25. And what is important – the tails of the distribution in the transverse planes are suppressed at 0.5 A, it means that electron current can be decreased further without sufficient particle loss in transverse direction.

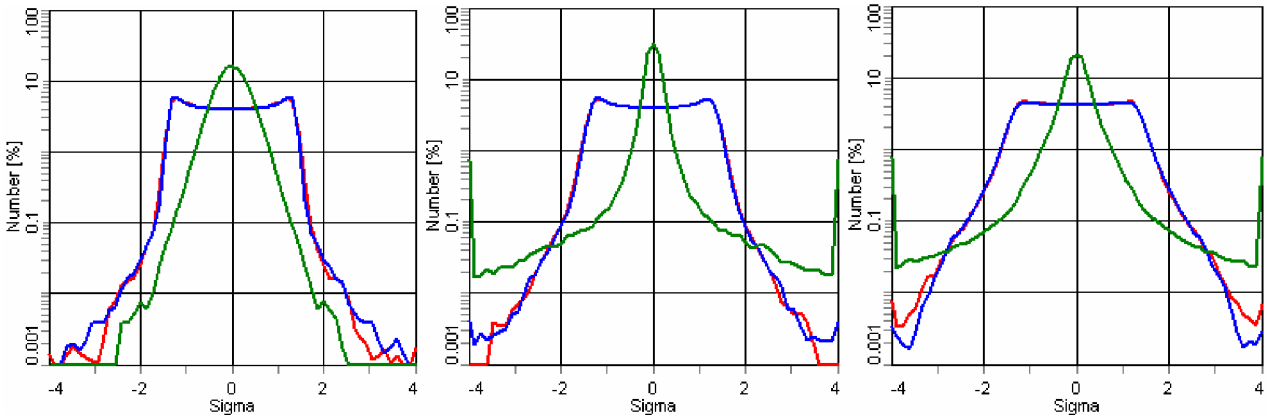

Fig. 25. Evolution of the equilibrium beam profile at increase of the heating power and decrease of the cooling pover. Left plot – electron current is 1 A, the target is switched off. Central plot – electron current is 1 A, the target is switched on. Right plot - electron current is 0.5 A, the target is switched on. HESR.

It should be noted that the simulations show that even 1 A of electron current can not prevent the formation of long tails in the distribution over momentum deviation. When the square containing 38% of the antiprotons lies in the range of below 10^{-5} in relative momentum deviation, the well pronounced tails have a width larger than 10^{-4}. It means that a serious attention has to be devoted to simulation of the tail population. The sufficient difference between profile widths in momentum space shows that even at emittance in the range of $10^{-8} \div 10^{-7}$ π·m·rad the intrabeam scattering can limit a minimum momentum spread. In the case of distribution with long tail the model used for IBS simulation is not valid. In all the existing in Betacool models the IBS is treated as a diffusion only, however for the particles at large velocities the friction inside the antiproton beam can play a sufficient role. And, of course, to predict real power of IBS heating a more adequate model of synchrotron motion is necessary.

Conclusions

As it shown in many experiments the electron beam misalignment is a powerful tool to control emittance of the ion beam. Its application for cooling at high resolution mode of HESR operation permits to stabilize the beam emittance at the level of $10^{-8} \div 10^{-7}$ π·m·rad (instead of 10^{-9} π·m·rad at perfectly aligned electron beam) and avoid sufficient increase of the momentum spread due to intrabeam scattering. Experiments at COSY, S-LSR and others shown, that increase of the beam emittance due to electron beam misalignment really leads to sufficient decrease of the momentum spread. Simulations of the antiproton dynamics in HESR demonstrates that application of the misalignment angle at the level of $(2 \div 3)\cdot 10^{-5}$ permits to achieve momentum spread at the level of 10^{-5} or even less.

General problem of the misalignment application in experiment with a pellet target is dramatic increase of peak to mean luminosity ratio in the case of chromatic instability development. In absence of the heating the particle distribution function in the space of oscillation amplitudes behaviors like delta function and the peak luminosity is determined by the particle density in the sharp edges of the distribution function. However, the simulations show that antiproton scattering inside the target prevents formation of very sharp edges of the distribution, and variation of the electron beam current permits to control the distribution shape. At optimum conditions one can hope to reach uniform distribution in the central part of the beam that is even more preferable than Gaussian one from the hand of peak to mean luminosity ratio.

One of the problems related with a pellet target application is a formation of long tails in the distribution function over momentum. The presented here simulations show that even at maximum design current the tails of the distribution function can contain a few percents of antiprotons. For realistic prediction of the tails evolution the algorithms for IBS and synchrotron motion simulations require sufficient improvement.

The synchrotron motion has to be simulated at more realistic model of RF bucket (including barrier RF bucket) with accurate simulation of the particle loss from the bucket. In reality the particles outside the bucket will be lost very fast due to mean ionization energy loss, correspondingly the tail width will be limited by the bucket height.

Simulation of IBS process has to be provided at arbitrary shape of the distribution function (in Betacool now only Gaussian and bi-Gaussian distribution can be simulated) and it has to take into account both effects related with the IBS – diffusion and friction (now IBS is treated as diffusion process only).